WILEY | Hindawi

Research Article

Metallocene Polyolefins Reinforced by Low-Entanglement UHMWPE through Interfacial Entanglements

Xin Tang,[1,2] **Jinheng Xing,**[2,3] **Xiang Yan** iD **,**[2,3] **Chunlin Ye,**[4] **Letian Zhang,**[4] **Yu Zhang,**[1,2]
Baoqiang Shu,[2] **Jingshan Mu,**[1] **Wei Li** iD **,**[1,2,3] **Jingdai Wang,**[2,3] **and Yongrong Yang**[2,3]

[1]*Department of Polymer Science and Engineering, School of Material Science and Chemical Engineering, Ningbo University, Ningbo, 315211 Zhejiang, China*
[2]*Ningbo Research Institute, Zhejiang University, Ningbo 315100, China*
[3]*Zhejiang Provincial Key Laboratory of Advanced Chemical Engineering Manufacture Technology, College of Chemical and Biological Engineering, Zhejiang University, Hangzhou 310027, China*
[4]*State Key Laboratory of Polyolefins and Catalysis, Shanghai Key Laboratory of Catalysis Technology for Polyolefins, Shanghai Research Institute of Chemical Industry Co., Ltd., No. 345 East Yunling Rd., Shanghai 200062, China*

Correspondence should be addressed to Xiang Yan; yanxiang028@zju.edu.cn and Wei Li; liwei2021@zju.edu.cn

By introducing low-entanglement UHMWPE, the mechanical properties of polyolefins are improved to varying degrees. For polypropylene, the lack of interaction between UHMWPE and polypropylene results in an unsatisfactory reinforcement effect, and the disentangled state makes it easier for the particles to form defects driven by a chain explosion. In contrast, regarding polyethylene and elastomer containing ethylene segments, low-entanglement UHMWPE plays a better role in reinforcement. A series of measurements including scanning electron microscopy (SEM), rheological measurements, differential scanning calorimetry (DSC), and mechanical measurement were used to investigate the mechanisms for the different enhancement effects. It originates from interdiffusion and entanglement forming of polyethylene segments across the interface, endowing the material with different aggregated and defect structures. For instance, EPDM possesses a higher optimal dosage of UHMWPE particles reflected in good interfacial interdiffusion with UHMWPE particles, leading to significant optimized mechanical performance.

1. Introduction

Metallocene-catalyzed polyolefin represents a revolutionary generation of petrochemical products with good toughness, impact resistance, transparency, and low odor [1]. Compared with the commonly used Ziegler-Natta catalysts, the metallocene catalysts possess the advantages of high catalytic activity, more applicable monomers, single active site, providing the polymer with uniform comonomer distribution, and reduced fraction of low-molecular-weight chains [2, 3]. Owing to the narrow molecular weight distribution (Mw/Mn = 2 to 3) of metallocene polyolefin, it exhibits good melt processability, high tensile strength, impact strength, and puncture resistance [4]. The metallocene polyolefin family includes different types of polyethylene (PE), polypropylene (PP), and ethylene copolymer. A variety of novel ethylene copolymer elastomers is invented, including metallocene EPDM, ethylene-octene copolymer (POE), and olefin block copolymers (OBCs), with the advantage of good affinity with conventional PE [5, 6].

Ultrahigh molecular weight polyethylene (UHMWPE) is a superior material concerning its exceptional toughness, low abrasion, and high impact resistance [7–9]. Nowadays, it is applied into the polymer composites to enhance the mechanical properties, such as toughness and tensile strength. The advantage of using UHMWPE particles is that the macromolecular chains at the surface are capable of reptating and entangling with the polymer matrix, in which

traditional inorganic particles are hard to bring about [10]. Interfacial bonding between a matrix and reinforcing particles is critical to determine the final mechanical properties of polymer blends.

Usually, a commercial UHMWPE is synthesized by a Ziegler-Natta catalyst at a high temperature (>60°C), where the chain growth rate is greater than the chain crystallization rate leading to the formation of many entanglements in the amorphous region [11]. An entangled UHMWPE (weight average molecular weight of 10^6 g/mol) chain exhibits a terminal relaxation time of 15 h at 180°C according to the reptation theory and the tube model [12], which shows that it is difficult for entangled UHMWPE segments to diffuse well into the matrix in the very limited shear rate and processing time. In contrast, the diffusion model of the low-entanglement material is different from that of entangled UHMWPE, which is presented in a chain explosion mode and is companied by a fast sideways motion [13, 14]. In our research group, Yang et al. has found that UHMWPE with the different entangled state has different effects on the structural and mechanical properties of HDPE/ UHMWPE blends. UHMWPE with a low-entanglement state is much easier to relax and overlap the adjacent HDPE chains, leading to more excellent mechanical behaviors [15].

For metallocene polyolefin, the use of ultrahigh molecular weight polyethylene for reinforcement is a very attractive attempt. To the best of our knowledge, there are rarely any reports concerning the reinforcement of metallocene polyolefins by low-entanglement UHMWPE particles. In addition, there is no study on the enhancement mechanism of UHMWPE-reinforced material from the perspective of interfacial interdiffusion. Therefore, we select three kinds of metallocene polyolefins containing different fractions of polyethylene segments (0%, 70.5%, and 100%) as PP, EPDM, and LLDPE. The synthesized nascent UHMWPE particles with a disentangled state based on our previous work is used for enhancement [16, 17]. We aim to observe the entanglement formation by the low-entanglement UHMWPE particles and the evolution of microstructures and mechanical properties through a series of investigations including scanning electron microscopy (SEM), rheological measurements, differential scanning calorimetry (DSC), and mechanical measurement.

2. Experiments

2.1. Materials. Metallocene polypropylene is supplied by Sinopec Group (China). EPDM (NORDEL™ IP 3722P) with 70.5 wt% of ethylene content, 29.0 wt% of propylene content, 0.5 wt% of ethylidene norbornene (ENB), and metallocene LLDPE (ELITE, 5401G) are purchased from Dow (USA). The low-entanglement ultrahigh molecular weight polyethylene (Dis-UHMWPE) with the melt flow rate (MFR) of 0.5 g/10 min (230°C, 21.6 kg) was synthesized based on our previous work [16]. Antioxidant (Irganox 1010) for Dis-UHMWPE is supplied by J&K Chemical Corp (China).

2.2. Blend Preparation. The weight fractions of Dis-UHMWPE particles melt-mixed into the metallocene poly-

olefin matrix are selected as 0 wt%, 1 wt%, 3 wt%, 5 wt%, 10 wt%, 20 wt%, 30 wt%, and 40 wt%. In addition, 0.6 wt% of antioxidant 1010 is added to prevent the oxidative degradation in subsequent experiments. The polymers were blended in the torque rheometer (HAPRO MIX-60, China) at 190°C for 5 minutes with a speed of 60 rpm. These blended samples are denoted as PP/U_x, PE/U_x, and $EPDM/U_x$, where x represents that the weight fraction of Dis-UHMWPE particles in the polymer blends is x wt%.

Afterwards, the blends were compressed under 10 MPa at 190°C for 5 minutes to produce samples by using the compression machine (XLB-HD, Dongfang Machinery Company, China). Samples were cooled down to the room temperature, and compressed dumbbell samples and disk samples were used for mechanical tests and rheological tests, respectively. The schematic diagram of blend preparation is shown in Figure 1.

2.3. Characterizations

2.3.1. Laser Particle Size Analysis. The dimensions of Dis-UHMWPE particles were determined by laser particle size analyzer (LS-230 Coulter, USA) with ethanol as dispersion medium. The principle of measurement was laser diffraction. The intensity of scattered light represents the number of particles with this particle size. In this way, the particle size distribution of the sample can be obtained by measuring the intensity of scattered light at different angles. The test results of particle size were D10, D50, and D90, which, respectively, indicated the particle size when the cumulative distribution was 10%, 50%, and 90% in the particle size volume distribution curve, and D50 was also called the average particle size.

2.3.2. Microscopic Observation. The morphology of Dis-UHMWPE particles was investigated by optical microscope (Leica DM500) with HD digital camera (ICC50W). The Dis-UHMWPE particles were spread evenly on the glass slide and then photographed by the aid of the digital camera.

The characteristics of fractures were performed by scanning electron microscopy (SEM, JEOL JSM-7500F). The three kinds of blends mentioned above were immersed into the liquid nitrogen for 15 minutes and then fractured into two pieces. To enhance the conductivity of the fracture surface of the material, the fractured sections were gold-sputtered before examining surface morphology.

2.3.3. Rheological Measurements. MFR measurement was conducted on the melt flow tester (HS-XNR-400A, Hesheng Company, China). The load during the experiment was selected as 2.16 kg. The piston and the tested polymer were preheated for 5 minutes and the temperature was kept at 230°C. The MFR value was recorded with the unit g/ 10 min. The melt flow index of each sample was tested at least two times, and the average values were taken.

The viscoelasticity of the blends was analyzed on a strain-controlled rheometer (HR10, TA Instruments, USA) with a parallel plate with a diameter of 20 mm. The dimension of disks for rheological tests were fixed at a diameter of 20 mm and a thickness of 2 mm. The disk between the
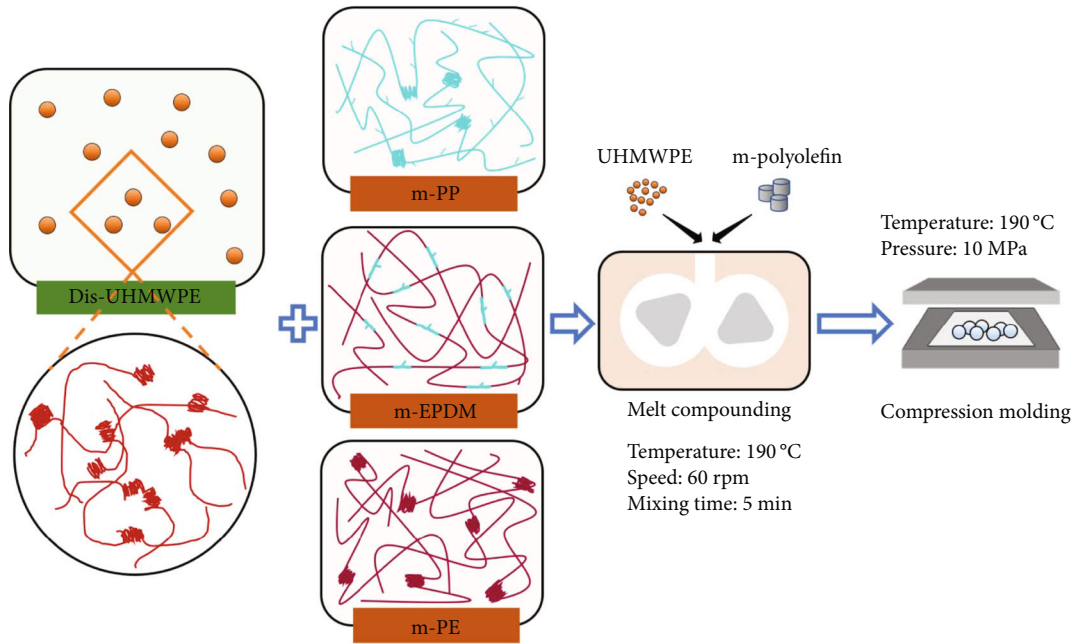
FIGURE 1: Schematic diagram of blend preparation.

parallel plates of the rheometer was heated to 190°C under a nitrogen environment, and the rheological measurements were performed on the oscillation mode. After waiting for 200 seconds to ensure the thermal stability of the sample, the rheological measurements were started. Frequency sweep tests of the blends were performed at a frequency range from 100 to 0.01 Hz with the strain amplitude of 1.0% in the linear viscoelastic regime.

The shear rate applied to the samples was linearly increased with the time from $0\,s^{-1}$ to $10\,s^{-1}$ and $18\,s^{-1}$, respectively. All samples were treated for 360 s. For the sake of convenience, the samples were named by the content of Dis-UHMWPE particles and the termination shear rate. For instance, PP/U_3-10 denotes that the content of Dis-UHMWPE particles was 3 wt% and the termination shear rate was $10\,s^{-1}$. Oscillation time sweep was carried out by the strain amplitude of 1.0% and the frequency of 5 Hz after the shear modification to track the reentanglement process of blends.

2.3.4. Thermal Behaviors. Thermal behaviors of the samples were recorded on differential scanning calorimetry (DSC) (TA DSC25, USA) in a nitrogen atmosphere. The samples were heated from 30°C to 190°C at a ramping rate of 10°C/min. Afterwards, five minutes were held to eliminate thermal history, and the samples were cooled to 30°C at the rate of 10°C/min. The temperature scan was repeated in the heating and cooling range between 30°C and 190°C at 10°C/min as the second cycle.

As for EPDM and LLDPE, crystallinity of LLDPE (X_{cPE}) was calculated by

$$X_{cPE} = \frac{\Delta H_m}{\Delta H_{PE0}} \times 100\%, \quad (1)$$

where ΔH_m is the melting enthalpy of the samples and ΔH_{LLDPE0} is the melting enthalpy of the fully crystalline polyethylene (293.0 J/g) [18].

As for PP blends, the crystallinity of PP was estimated by the second cooling curve using

$$X_{cPP} = \frac{\Delta H_{mPP}}{(\Delta H_{PP0} \times \omega_{PP})} \times 100\%, \quad (2)$$

where ΔH_{mPP} is the enthalpy of cooling crystallization of PP during the second cooling process, ΔH_{PP0} is the melting enthalpy of 100% crystalline PP, which was taken to be 209 J/g [19], and ω_{PP} is the weight fraction of PP component in the blend.

Similarly, the crystallinity of UHMWPE in PP blends was estimated by using

$$X_{cUHMWPE} = \frac{\Delta H_{mUHMWPE}}{\Delta H_{PE0} \times \omega_{UHMWPE}} \times 100\%, \quad (3)$$

where $\Delta H_{mUHMWPE}$ is the enthalpy of cooling crystallization of UHMWPE during the second cooling process and ω_{UHMWPE} is the weight fraction of UHMWPE component in the blend.

2.3.5. Mechanical Tests. The tensile tests were carried out on an electromechanical universal test system (Model 5566, Instron, USA) at room temperature (25°C) with a tensile speed of 50 mm/min. The dumbbell splines were produced with the length, width, and thickness of 30 mm, 5 mm, and 2 mm, respectively. For each group of tests, more than four samples were tested, and the average values and standard deviations were recorded.

The hardness of EPDM/U, PP/U, and LLDPE/U was measured by using a Shore hardness tester (Shore "D").

The specimens were placed on a flat plane. The indenter of the hardness tester was then pressed on the samples without any vibration, making sure that it was parallel to the surface. The tested values must be recorded within 1 second after the indenter and the samples were fully touched. Each type of samples was measured for five times at different position and the average values were taken.

3. Results and Discussion

3.1. Morphology and Distribution of Dis-UHMWPE Particles. The mean diameters of Dis-UHMWPE particles investigated by laser particle size analysis and their morphology are shown in Figure 2. The mean diameter D50 of Dis-UHMWPE particle is close to $135 \mu m$, which corresponds well with the images taken under an optical microscope. Dis-UHMWPE nascent particles of different particle sizes are typically "grape-shaped," which are directly composed of loosely stacked nodular particles [20]. Compared with highly entangled UHMWPE, the size of nodular particles of Dis-UHMWPE is generally smaller, and different numbers of nodular particles agglomerate to form new particles of different sizes.

These UHMWPE particles were incorporated into different metallocene polyolefin matrices. The SEM images of fractured sections of the melt-processed blends are illustrated in Figure 3. After the melt processing, the Dis-UHMWPE particles have undergone a significant evolution. It reflects the biphasic miscibility of the blends and distribution of UHMWPE particles. When the concentration is low, a relatively homogeneous system is formed without observable particles. As for PP/U, obvious particles appear when the UHMWPE content is 3 wt%. As the content of UHMWPE increases, tremendous particles gradually appear on the surface indicating deteriorated miscibility, especially when 10 wt% of Dis-UHMWPE particles are incorporated, with the volume average diameter of $0.9 \mu m$. In contrast, the frequency of appearance of UHMWPE particles in EPDM and LLDPE is significantly lower compared with PP/U samples, even if the addition content of Dis-UHMWPE particles reaches 10 wt%. Meanwhile, the volume average diameter of the UHMWPE particles is increased in EPDM reaching $4.1 \mu m$ due to varied surface tension and rheological properties of different blending systems.

The fracture section of LLDPE/U in Figure 3 presents a clear three-dimensional network structure. When the addition content of Dis-UHMWPE particles reaches more than 5 wt%, as shown in Figures 3(c_5) and 3(c_{10}), obvious particles begin to appear on the fractured surface. 90% of UHMWPE particles are concentrated in $0.5\text{-}1.0 \mu m$ with the volume average of $0.6 \mu m$ exhibiting good mixing characterist. SEM results intuitively provide a judgment of biphasic miscibility. Based on the above-mentioned observation, it is concluded that when the Dis-UHMWPE particles are mixed with the polyolefin, the nodular particles are separated and physically interacted with the matrix, of which the schematic figure is shown in Figure 3(e). It exhibits different particle sizes of UHMWPE based on the choice of polymer matrix and addition content of Dis-UHMWPE

particles. Furthermore, from the perspective of the macromolecular chain segments, the interfacial interdiffusion between the UHMWPE particles and the polyolefin matrix needs to be revealed.

3.2. Interfacial Interdiffusion. The melt flow rates (MFR) and its normalized values of the polymer blends are illustrated in Figure 4. EPDM performs relatively weak fluidity compared with PP and LLDPE. In addition, the introduction of Dis-UHMWPE particles gradually decreases the fluidity of the polyolefin matrix. The content of Dis-UHMWPE particles should be controlled within a low range to ensure sufficient melt processing performance. When the addition amount of UHMWPE is 10 wt%, the fluidity reduction ratio of LLDPE and EPDM is very similar, approximately approaching 64%. Meanwhile, the PP blend shows 30% attenuation of melt flow index. It hints different interfacial affinity with UHMWPE of polypropylene and polyolefin containing polyethylene segments.

The miscibility and interdiffusion behaviors of blends with different weight fraction of UHMWPE are evaluated by high-temperature dynamic frequency scanning. Taking the samples with 1 wt% UHMWPE as an example, as shown in Figure 4(c), in the high frequency regime, the storage modulus (G') of the blends is greater than the loss modulus (G''). Materials tend to behave more like solid under high frequency stimulation due to oscillatory shear deformation, where it is over the crossover frequency with inability in the motion of entire molecular chains. By comparing the change of the crossover frequency of the blends, we understand the effect of the UHMWPE content on relaxation behavior. As shown in Figure 4(d), with the increase of UHMWPE content, the crossover frequency gradually decreases and longer relaxation time is required. LLDPE matrix is more sensitive to UHMWPE changes, and the liquid-like to solid-like transition shifts quickly to low frequencies. It originates from the formation of networked structures with the incorporation of Dis-UHMWPE [21–23].

As shown in Figure 5, the viscosity of the blends increases gradually with the increment of UHMWPE fraction, which results from the hindrance by the ultralong molecular chain of UHMWPE [18]. EPDM exhibits higher viscosity compared with PE, corresponding well with the MFR results. The LLDPE/U and EPDM/U show a relatively high complex viscosity compared with the pristine ones, demonstrating that the introduction of Dis-UHMWPE particles improves the intermolecular entanglements of the blends and shows long-period relaxation behavior [24]. The LLDPE/U and EPDM/U exhibit a typical shear thinning behavior in contrast to the apparent Newtonian behavior regime of pure LLDPE, which is beneficial for melt processing at high shear rate. Figures 5(b)–5(e) present the evolution of storage modulus of EPDM/U and LLDPE/U blends with different UHMWPE content. The storage modulus represents the elasticity of the melt and the relaxation behaviors of the molecular chains. As shown in the storage modulus versus frequency curves, the blended samples have larger modulus at low shear frequency compared with pristine samples, which is ascribed to the longer relaxation time.
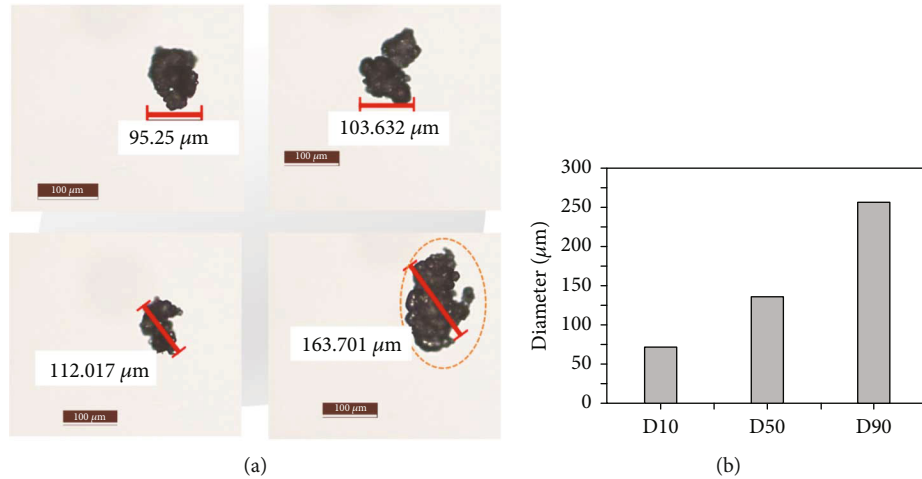
(a)　　　　　　　　　　　　　　(b)

Figure 2: (a) Morphology of Dis-UHMWPE particles. (b) Mean diameters of Dis-UHMWPE particles in cumulative distribution of 10%, 50%, and 90%.

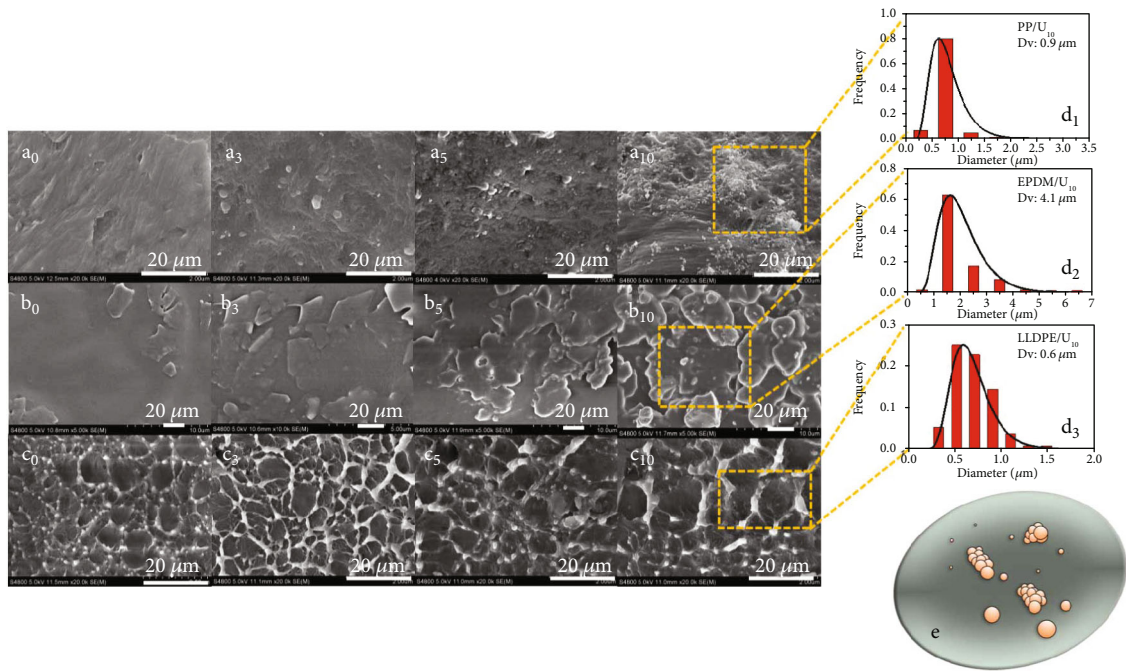Figure 3: SEM images of fractured sections of three kinds of blends. (a_0, a_3, a_5, a_{10}) PP-$U_{0,3,5,10}$. (b_0, b_3, b_5, b_{10}) EPDM-$U_{0,3,5,10}$. (c_0, c_3, c_5, c_{10}) LLDPE-$U_{0,3,5,10}$. (d_1, d_2, d_3) Particle size distribution of PP/-U_{10}, EPDM-U_{10}, and LLDPE-U_{10}. (e) Schematic figure of blending process of polyolefin with Dis-UHMWPE particles.

The change of modulus for EPDM/U is negligible compared to that of LLDPE/U when the UHMWPE fraction is less than 10 wt%. With the further increase of UHMWPE concentration, the storage modulus is improved significantly at low frequency region ranged from 0.01 Hz to 0.1 Hz, which means that a large amount of entanglement points and mechanical network between UHMWPE chains and the adjacent chains are formed.

Loss tangent (tan δ) is an important parameter to measure the viscoelastic transition of melt, illustrating the balance between energy loss and storage. The smaller tan δ corresponds to the better elasticity [25]. A relative apparent

positive slope occurs in the EPDM/U blend at low shear frequency (Figure 5(c)), which is attributed to the interface strength effect between EPDM and UHMWPE by forming tight entanglement networks [26]. Compared with EPDM/U, tan δ of LLDPE/U decreases more obviously with the increase of frequency, indicating viscous fluid behavior and less pronounced elasticity [27]. In summary, UHMWPE has a great influence on the viscoelasticity of EPDM and LLDPE by forming a certain degree of entanglements.

To gain a deeper understanding of the miscibility of the two polymers, the above-mentioned data is remapped in Figure 6. The log-additivity rule is a common method to
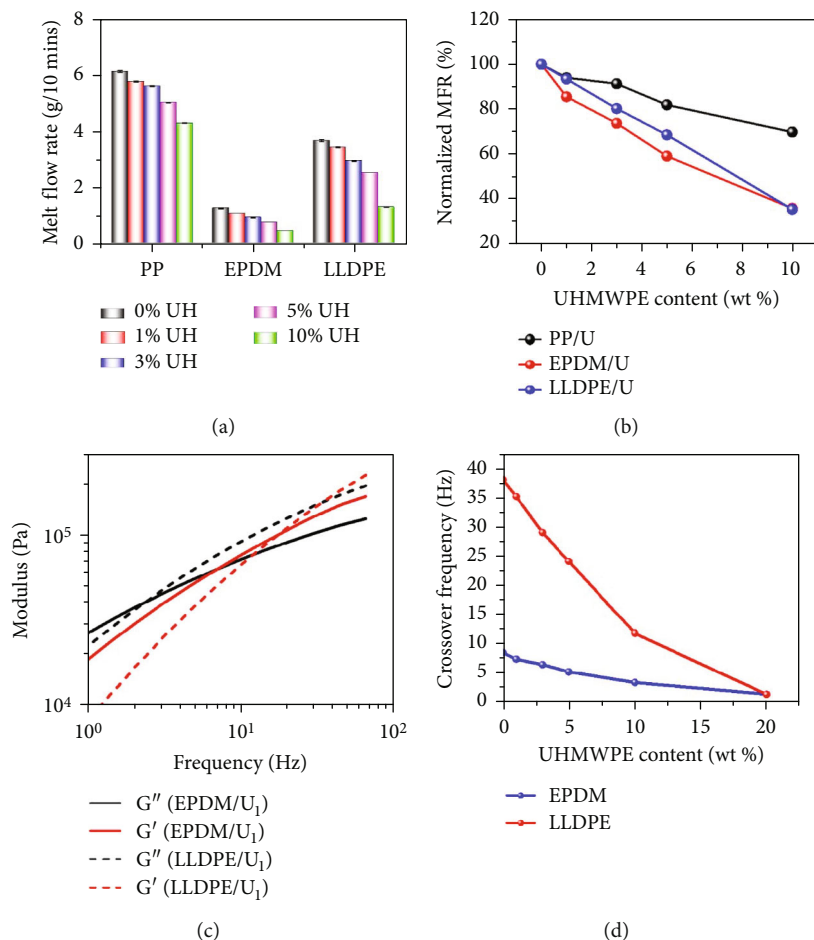
(a)

(b)

(c)

(d)

FIGURE 4: (a) Melt flow rate of three blends. (b) Normalized MFR (melt flow rate) of three blends. (c) Modulus versus frequency at 190°C for EPDM/U1 and LLDPE/U1. (d) Crossover frequency versus UHMWPE content at 190°C for EPDM/U and LLDPE/U.

analyze the miscibility of biphasic blends [28]. Figures 6(a)–6(d) show the variation of complex viscosity and storage modulus at 0.01 Hz versus UHMWPE content at 190°C for EPDM/U and LLDPE/U. Compared with LLDPE/U, EPDM/U exhibits obviously higher linearity in the curves concerning the linear variation of log $G'_{(0.01\,Hz)}$ and log $\eta_{(0.01\,Hz)}$ versus UHMWPE content. It indicates that the biphasic miscibility of EPDM/U blend is more impressive than that of LLDPE/U.

Cole-Cole curve is an empirical correlation tool to analyze the miscibility of the blends, which illustrates the relationship between real viscosity (η') and imaginary viscosity (η''). The degree of downward bending of Cole-Cole curves represents phase separation and relaxation process of dispersed particles [29], of which the smooth semicircle represents good miscibility [30, 31]. As shown in Figure 6(f), the LLDPE matrix and UHMWPE with the content below 3 wt% exhibit good miscibility reflected in observable semicircles. The shape of the curve sharply deviates from the semicircle to a straight line with an upturn tail at the concentration of 10 wt% due to deteriorated biphasic miscibility. In contrast, the Cole-Cole curve of pristine EPDM is slightly bent due to its intrinsic structure of hard blocks of polyethylene

segments and soft blocks of polypropylene segments. There is violent phase separation with an upturn tail in the curve when the addition fraction of Dis-UHMWPE particles exceeds 20 wt%.

The variation of Han curves with different compositions also indicates the phase separation behavior based on molecular viscoelasticity theory [32]. The obvious difference between heterogeneous polymer system and homogeneous polymer system lies in whether there exists composition dependence. If there is no composition dependence, the polymer melt is homogeneous. Therefore, it proves that there is no distinctive phase separation in melt state when the fraction of UHMWPE in EPDM/U is below 10 wt%. In contrast, for the LLDPE/U system, the Han curve has a significant deviation within the fraction of 10 wt%, which shows that the obvious phase separation occurs in the melt state. When the content of UHMWPE exceeds 10 wt%, LLDPE/U blends exhibit perceptible composition dependence, which is ascribed that a large amount of UHMWPE is difficult to be well miscible with the matrix. Meanwhile, regarding better miscibility, the maximum addition threshold of Dis-UHMWPE particles for EPDM reaches 20 wt%, which corresponds well with Cole-Cole curves. In terms of rheology, the maximum addition amount of blending
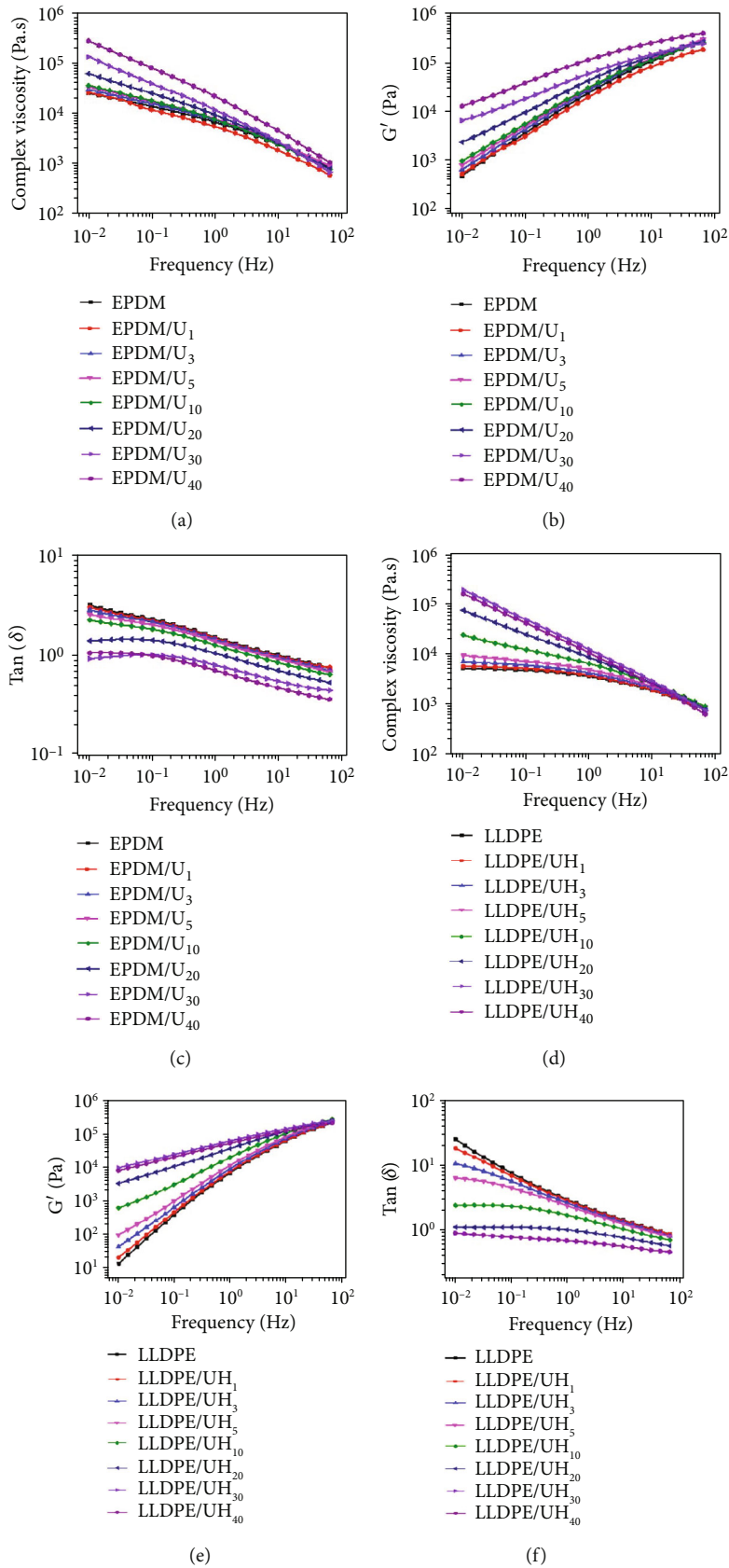
Figure 5: (a, d) Complex viscosity versus frequency at 190°C for EPDM/U and LLDPE/U. (b, e) Storage modulus versus frequency at 190°C for EPDM/U and LLDPE/U. (c, f) Tan δ as functions of frequency at 190°C for EPDM/U and LLDPE/U.
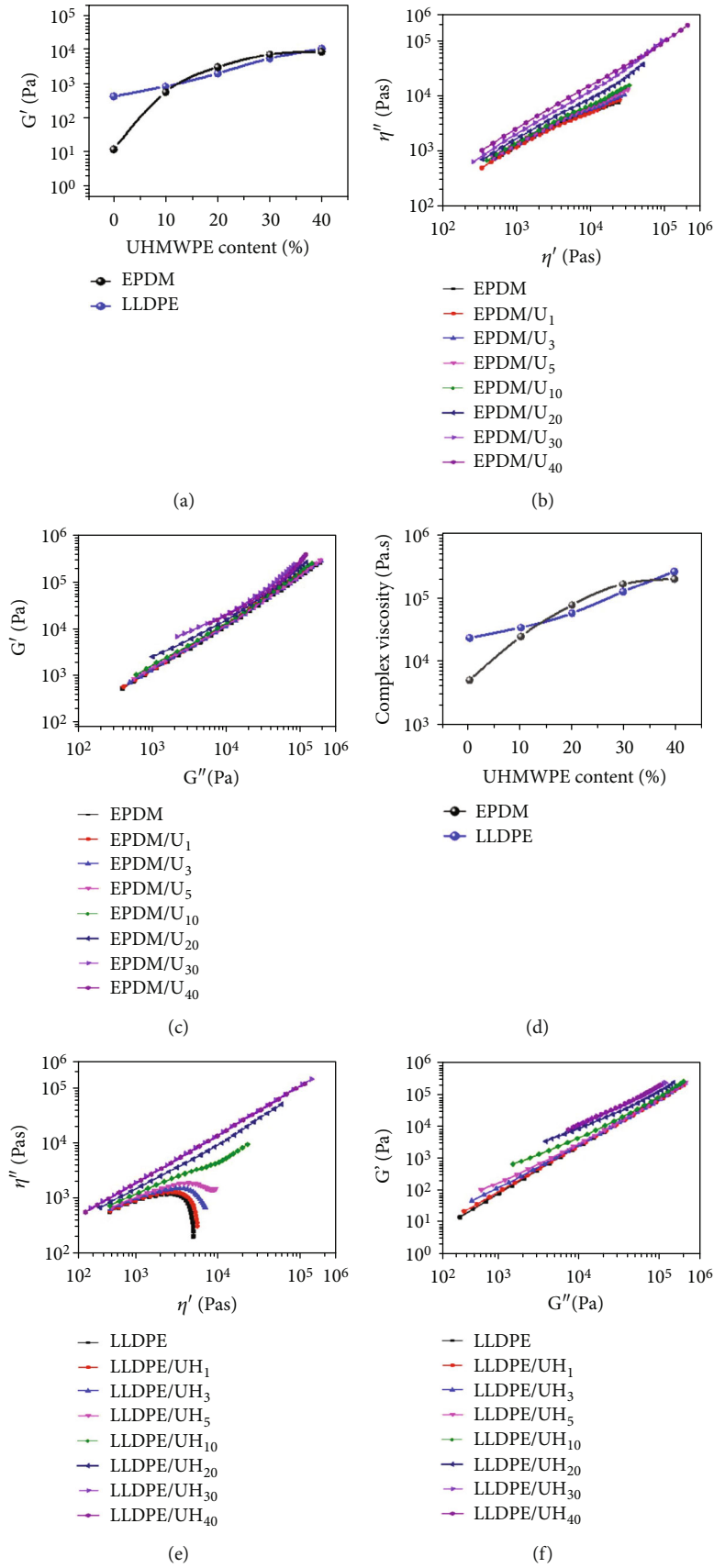
(a)

(b)

(c)

(d)

(e)

(f)

Figure 6: (a, d) Variation of storage modulus and complex viscosity at 0.01 Hz versus UHMWPE content at 190°C for EPDM/U and LLDPE/U. (b, e) Cole-Cole curves for EPDM/U and LLDPE/U. (c, f) Han curves for EPDM/U and LLDPE/U.
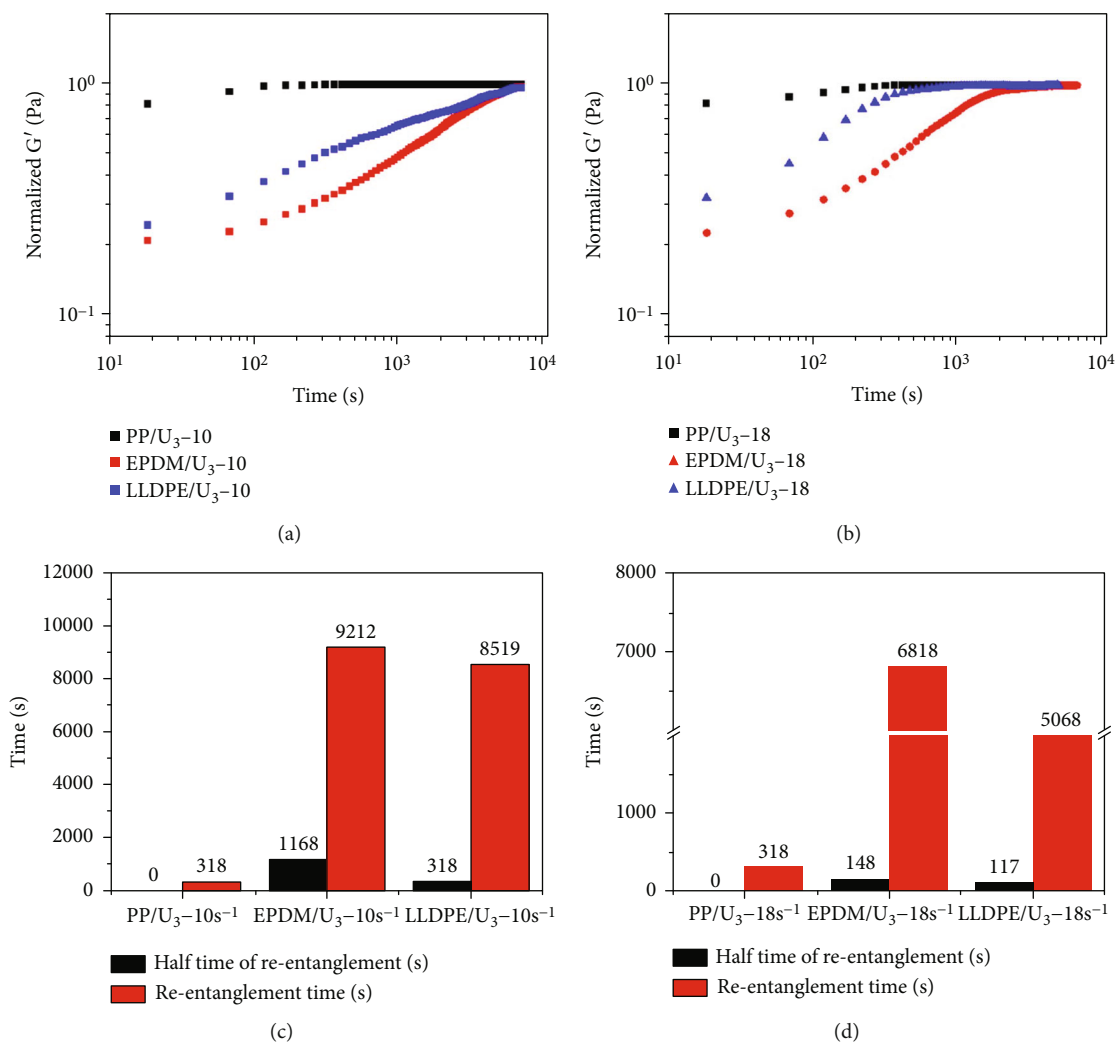
FIGURE 7: (a, b) Buildup of normalized storage modulus of selected samples with time at 190°C. Half time of reentanglement and reentanglement time after shear modification: (c) terminal shear rate: $10\,s^{-1}$ and (d) terminal shear rate: $18\,s^{-1}$.
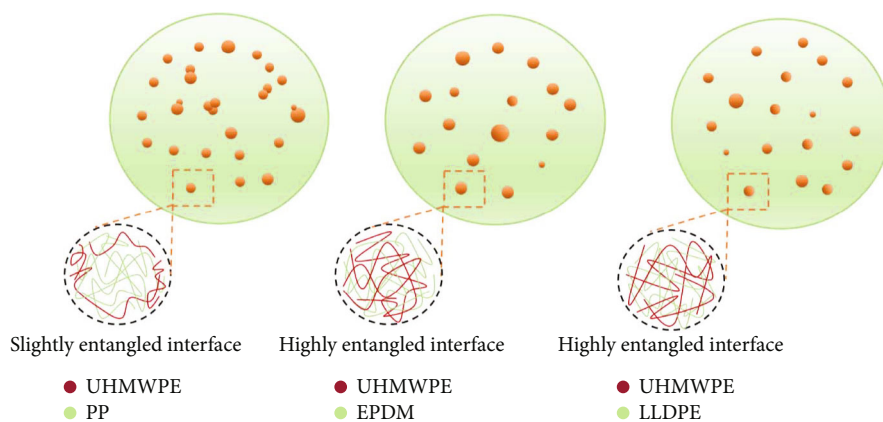

FIGURE 8: Interfacial interdiffusion of PP/U, EPDM/U, and LLDPE/U blends.

(a)

(b)

(c)

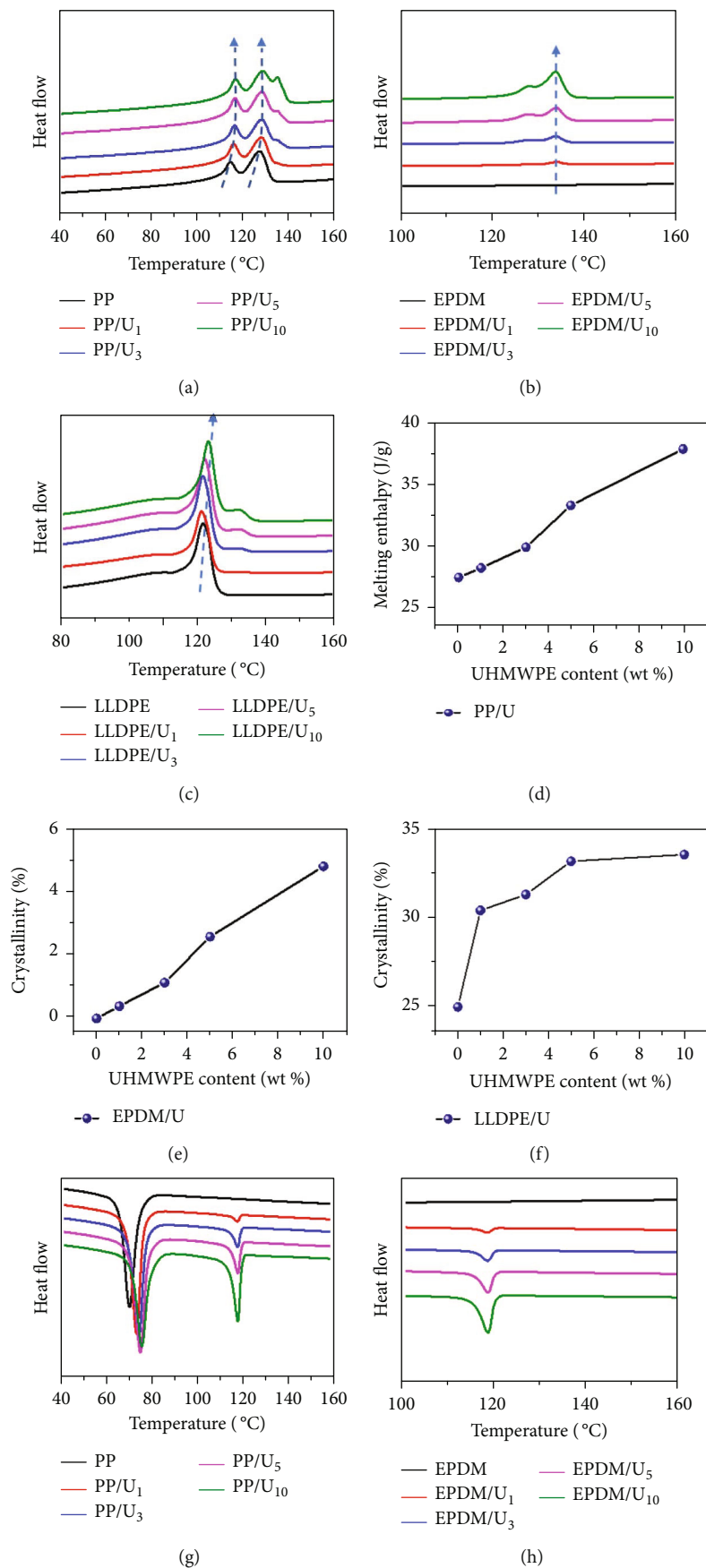

(d)

(e)

(f)
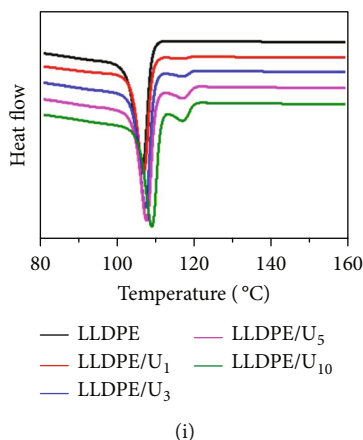

(g)

(h)

Figure 9: Continued.

(i)

FIGURE 9: DSC curves of three kinds of blends. (a–c) The second heating scan of PP/U, EPDM/U, and LLDPE/U. (d) Melting enthalpy of PP/U. (e, f) The crystallinity of EPDM/U and LLDPE/U. (g–i) The second cooling scan of PP/U, EPDM/U, and LLDPE/U.

modification is 10 wt% and 20 wt% for LLDPE and EPDM, respectively.

Different from nanoparticles, the molecular chains of UHMWPE are disentangled under the shear modification, and the disentangled chain segments tend to reentangle to equilibrium state in the form of random coil originated from the entropy driven in the molten state [33]. Therefore, we use rheological methods to track the recovery process of entanglement, reflecting the situation of biphasic interfacial interdiffusion. Figures 7(a) and 7(b) record the recovery process of storage modulus of the biphasic blends versus time after reaching the terminal shear rates of $10 s^{-1}$ and $18 s^{-1}$, in logarithmic form, respectively. The recovery process is generally divided into two stages including chain explosion stage and reptation stage, respectively [34]. In the chain explosion stage, the chain segment moves and forms large number of physical entanglement nodes rapidly. Subsequently, the motion of the chain segment is greatly limited in the reptation stage, and it takes a long time to reach the platform. We define the time for the storage modulus to recover to half equilibrium and total equilibrium as half reentanglement time and reentanglement time, respectively, and the related data are illustrated in Figures 7(c) and 7(d). PP/U blends only takes 318 s to reach the equilibrium state, which shows that the chain segments of Dis-UHMWPE particles do not effectively diffuse into the chain segments of PP matrix existing in the form of agglomeration. After shear modification, the chain segments of PP quickly return to equilibrium under the action of entropy drive. The interfacial interdiffusion between UHMWPE and PP is very weak compared with the other two polymer blends, and it is difficult to form an effective entanglement network to retard the recovery process which is still dominated by the PP molecular chains.

Two different shear rates are selected to track the differences, and the order of recovery time among different materials remains unchanged, reflected in significantly shorter recovery time of PP/U and prolonged time of LLDPE/U and EPDM/U. It is attributed that the motion of these two polymers is greatly constrained by UHMWPE,

and the longer recovery time probably corresponds to better interfacial interdiffusion. Molecular chains of UHMWPE diffuse into the molecular chains and form entanglement networks with EPDM and LLDPE. In detail, when the terminal shear rate is $10 s^{-1}$, EPDM/U_3 takes 1168 s to reach the semi-equilibrium state, almost four times that of LLDPE/U_3. It gives evidence that the interaction between EPDM and UHMWPE is strong enough to form entanglements between polyethylene segments.

Based on these findings, the structure diagram of the UHMWPE-containing blends with different polyolefin is given in Figure 8. There are weakly any strong intermolecular forces between PP and UHMWPE with slightly entangled interface. For LLDPE and EPDM, there exists some degree of intermolecular diffusion of UHMWPE towards the polyolefin matrix forming entanglements between molecular chains. Although there are relatively larger particles of EPDM in the matrix, the interdiffusion force of UHMWPE into EPDM matrix is still very strong due to the presence of a large fraction of polyethylene segments.

3.3. Crystallinity.
Figure 9 illustrates the second heating and cooling curves of the blends in the DSC tests, where the related data regarding crystallinity are presented in Figures 9(d)–9(f). The cooling curves of the first cycle and the second cycle almost coincide, indicating that the thermal history of the blends has been effectively eliminated. The melting enthalpy of PP/U is gradually increased with the addition of Dis-UHMWPE particles. It is mainly due to enhanced crystallization ability and high melting enthalpy for 100% crystalline polyethylene segments. The crystallinity of PP (low-temperature peak) is estimated from the cooling process (Figure 9(g)) ranging from 13.3% to 14.5%, while the crystallinity of UHMWPE (high-temperature peak) is from 31.9% to 35.8%. Although the crystallinity of PP does not change much, its crystallization temperature is significantly advanced from 70.0°C for pristine PP to 73.2°C for PP/U_1, where UHMWPE plays the role of a nucleating agent. The two melting peak temperatures of pristine PP (Figure 9(a)) are 114.3°C and 127.2°C, representing two kinds of conformations in PP. The low-temperature peak and high-
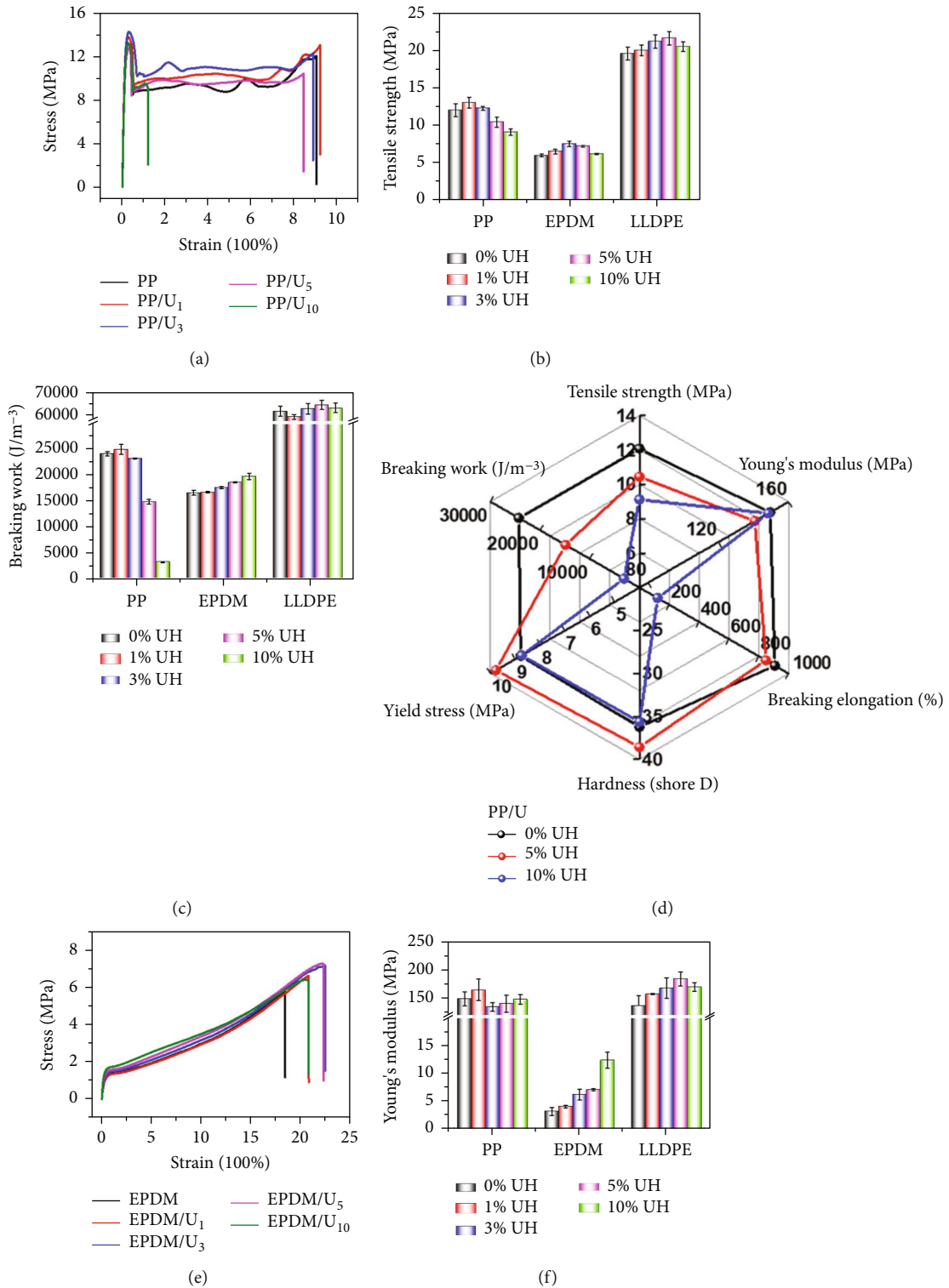
(a)

(b)

(c)

(d)

(e)

(f)

FIGURE 10: Continued.
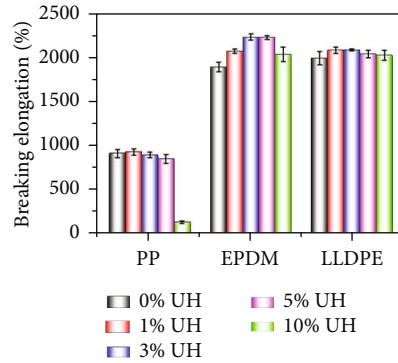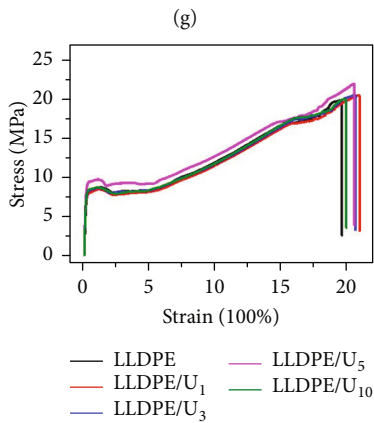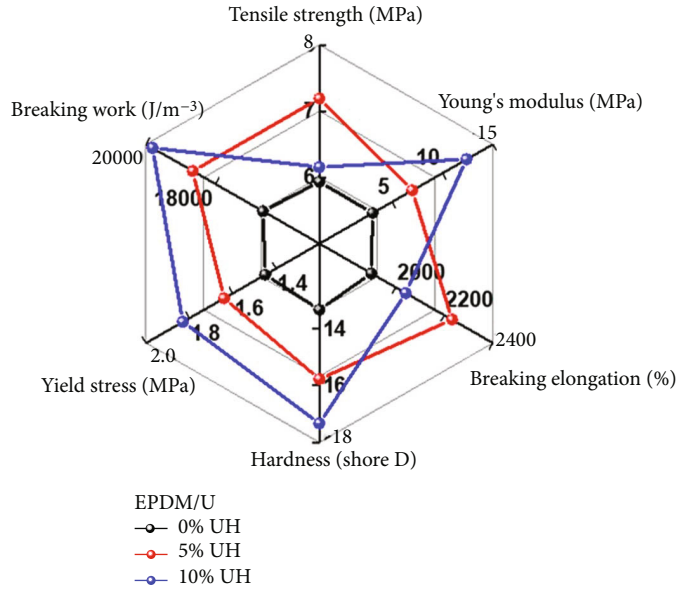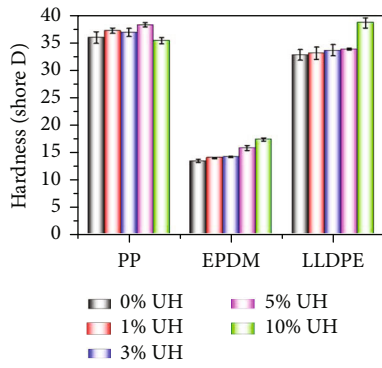
(g)

(h)

(i)

(j)

(k)

(l)
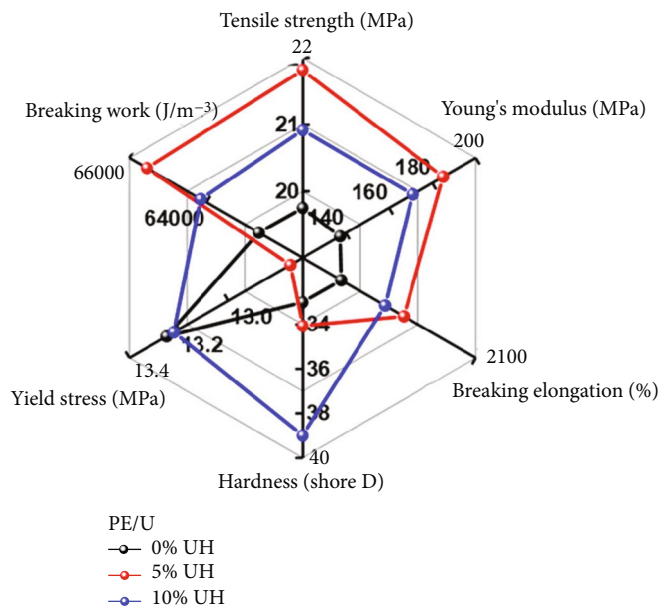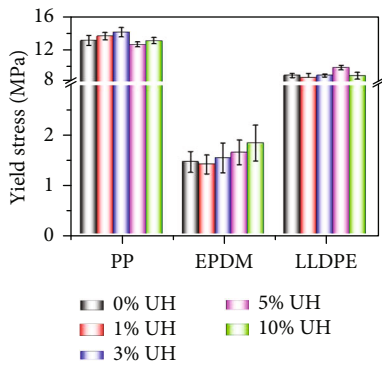
FIGURE 10: (a, e, i) Typical stress-strain curves of three samples, (b) tensile strength, (c) breaking work, (f) Young's modulus, (g) hardness, (j) breaking elongation, (k) yield stress, (d) radar chart of PP/U blend, (h) radar chart of EPDM/U blend, and (l) radar chart of LLDPE/U blend.
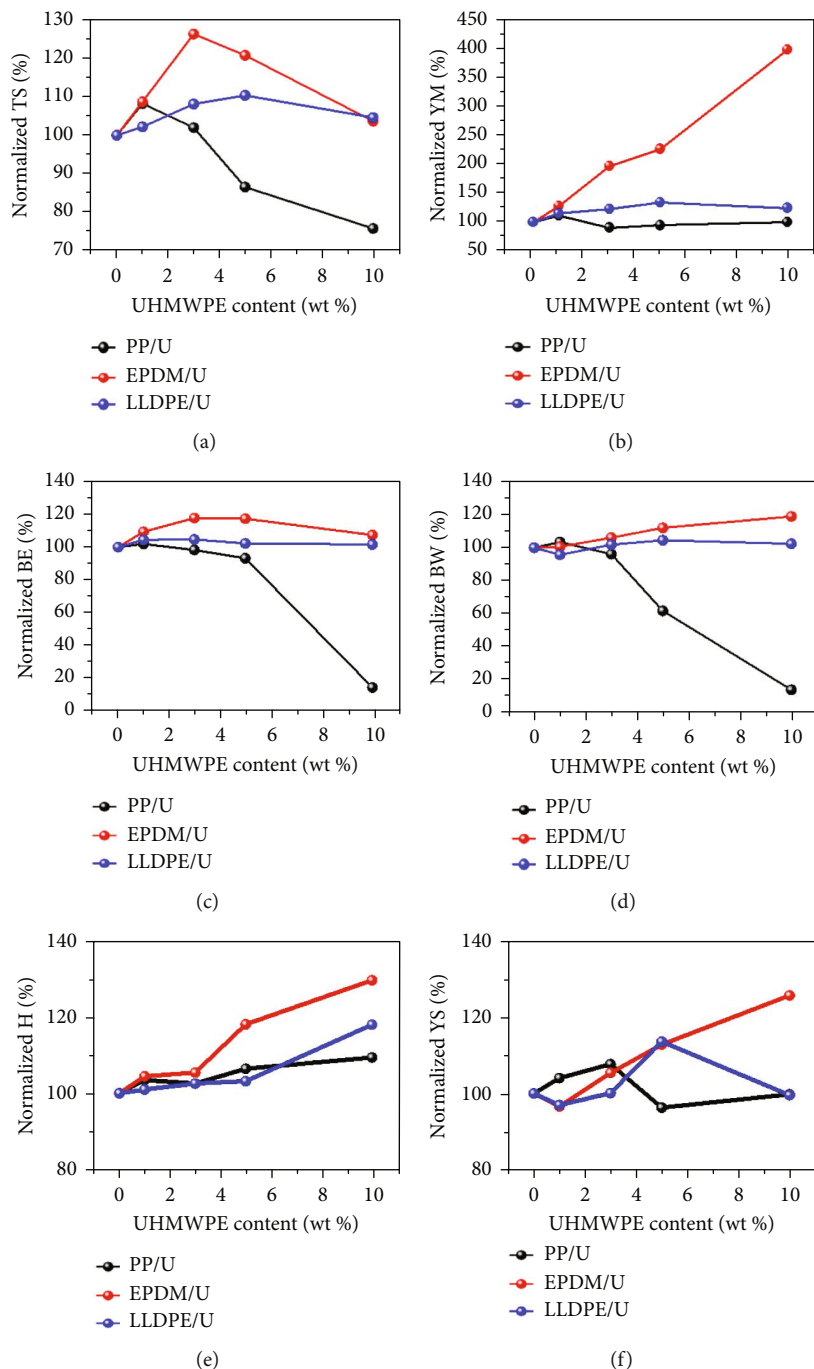
FIGURE 11: Normalized diagram of mechanical properties: (a) tensile strength (TS), (b) Young's modulus (YM), (c) breaking elongation (BE), (d) breaking work (BW), (e) hardness (H), and (f) yield stress (YS).

temperature peak represent isotactic PP and syndiotactic PP, respectively. Two peaks of PP/U samples have 1°C shift to a higher temperature. Meanwhile, there appears a shoulder peak of UHMWPE at 134.5°C when the addition amount of UHMWPE is greater than 3 wt%. As a nucleating agent, UHMWPE does not participate in the cocrystallization process of PP and only slightly improves the aggregated structure of PP. It increases the melting point of PP without significantly impacting its crystallinity.

EPDM with an ethylene content of more than 65% is often classified as crystallizable products as semicrystalline. When there is no UHMWPE in the EPDM matrix, the polymer does not crystallize without obvious melting points, because methyl groups from propylene units interrupt crystallization of EPDM. The situation is changed when Dis-UHMWPE particles are incorporated. The melting points of UHMWPE usually exceed 130°C [35]. When Dis-UHMWPE particles are incorporated into the matrix, the
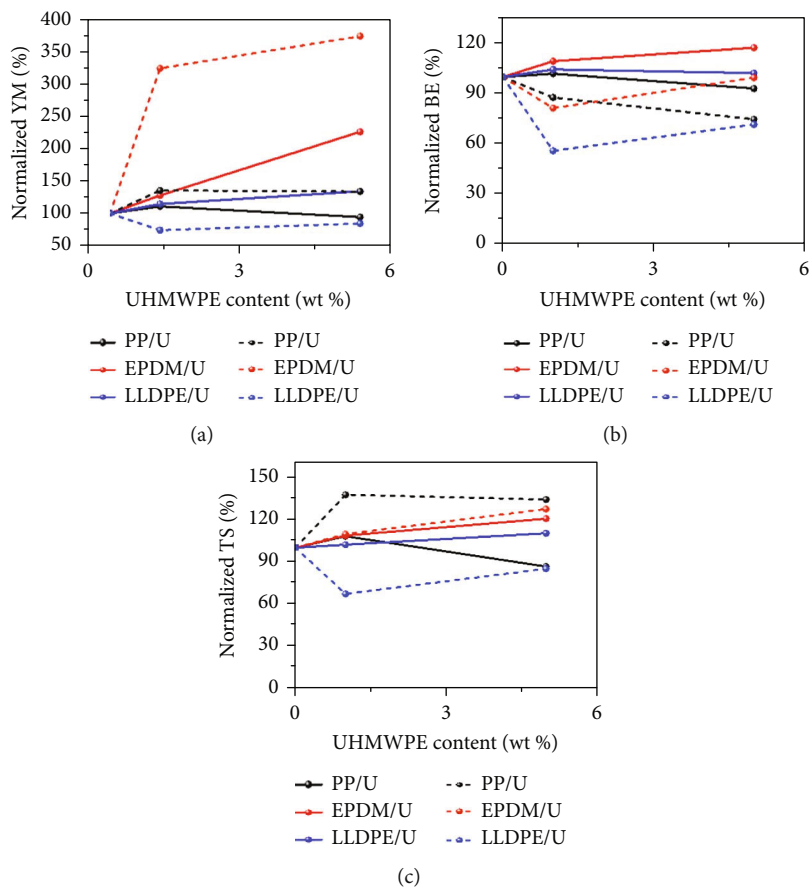
(a)

(b)

(c)

FIGURE 12: Normalization mechanical properties of three kinds of samples blended with low-entanglement UHMWPE (solid line) and high-entanglement UHMWPE (dashed line): (a) Young's modulus, (b) breaking elongation, and (c) tensile strength.

melting point of UHMWPE content in the blend is approximately 133.8°C. In addition, there appears a shoulder peak at 128.2°C, which is ascribed to the crystallization of polyethylene segments from EPDM. The incorporation of Dis-UHMWPE particles promotes the nucleation process and growth of the crystallization process [36, 37]. During the cooling process, the blend cocrystallizes at 118.3°C, which gives evidence of good interfacial interdiffusion between EPDM and UHMWPE. The overall crystallinity of the EPDM/U is slightly increased with the addition of UHMWPE, remaining a low level within 5%, ensuring that EPDM retains the characteristics of rubber.

In Figure 9(i), there is no obvious cocrystallization between LLDPE and UHMWPE. However, the melting peak of LLDPE/U blends is shifted from 122.3°C to 128.2°C (Figure 9(c)), which is illustrated that the crystallization behaviors are greatly affected by the addition of UHMWPE. Similarly, the melting point of UHMWPE is close to 133.8°C. It is worth noting that a small amount of UHMWPE results in great change for crystallinity of LLDPE. When 1 wt% of Dis-UHMWPE particles are incorporated, the crystallinity is increased from 24.9% to 30.4% as shown in Figure 9(f). When the addition amount is further enhanced, the increment in crystallinity becomes very small, which is distinct from the crystallization behavior of EPDM. As shown in Figure 9(e), EPDM has a stable increase

in crystallinity within a larger content range, which is due to its high filling threshold and good interdiffusion with UHMWPE.

3.4. Mechanical Performance.
The typical stress-strain curves of three series of blends are shown in Figure 10. PP and LLDPE exhibit the mechanical performance of ductile materials with very high breaking elongation. At the beginning of stretching, stress-strain curves show a sharp slope which represents general elastic deformation till the yield point, followed by necking and cold drawing during which LLDPE exhibits the strain hardening behavior. As for EPDM, it acts as a typical elastomer without necking.

The mechanical properties of the three blends, including tensile strength, breaking elongation, Young's modulus, hardness, yield stress, and breaking work, are also presented in Figure 10. The mechanical properties of PP/U blends are enhanced only when the amount of UHMWPE is tiny (1 wt%). When the addition amount is further increased, there is a sharp decline in the tensile strength, breaking elongation, and breaking work. Its Young's modulus, hardness, and yield strength basically keep unchanged. From the radar chart, it shows that in the biphasic system, UHMWPE is not suitable for enhancing the mechanical properties of PP. It is mainly ascribed that the crystalline structure of PP remains basically unchanged, and the addition of UHMWPE

presents in the PP matrix in the form of defects leading to stress concentration, which corresponds well with the SEM results.

In contrast, as shown in Figure 11, Dis-UHMWPE particles have significantly better reinforcement effects on LLDPE and EPDM. As for LLDPE/U blends, 5 wt% of UHMWPE successfully improves the comprehensive mechanical performance compared with pristine LLDPE, especially tensile strength by 11%, yield strength by 11%, and hardness by 5%. Meanwhile, the breaking elongation is slightly decreased compared with LLDPE/U$_3$, which may be ascribed to deteriorated miscibility as the UHMWPE content increases. As for EPDM, when the addition amount of UHMWPE into EPDM is 5 wt%, the enhancement effect in mechanical performance is significant, including tensile and yield strength, breaking elongation and work, Young's modulus, and hardness. When the addition amount reaches 10 wt%, Young's modulus is dramatically enhanced from 3.1 MPa to 12.4 MPa by 3 times. Meanwhile, its yield strength, hardness, and breaking work are continuously enhanced, and the related values are increased by 26%, 30%, and 19%, respectively. It hints that UHMWPE plays an excellent role in enhancement in EPDM, originated from the good interfacial interdiffusion and promoted aggregate structure caused by cocrystallization.

In order to highlight the difference between low-entanglement UHMWPE and high-entanglement one, we also tried to add high-entanglement UHMWPE into the polyolefin matrix for comparison. As shown in Figure 12, compared with the high-entanglement UHMWPE, low-entanglement UHMWPE has a more significant effect on improving the mechanical properties of polyethylene. This is because the structure of the low-entanglement UHMWPE entanglement network is looser, and the chain segments of LLDPE are easier to enter the inner part of the low-entanglement UHMWPE chain. From the previous analysis, UHMWPE exists in the PP matrix in the form of defects, and the low-entanglement UHMWPE is more prone to chain explosion than the high-entanglement UHMWPE. Therefore, the low-entanglement UHMWPE will form larger defects during the blending process, resulting in the degradation of the mechanical properties of PP/U. In contrast, highly entangled fillers form smaller-scale defects. So for low-entanglement UHMWPE, we have to distinguish its application scenarios. It is aimed to form better entanglement between UHMWPE and the matrix, and we need to ensure that the filler does not reentangle itself during the blending process.

4. Conclusion

The interfacial interdiffusion and mechanical evolution of metallocene polyolefins by introducing low-entanglement UHMWPE particles have been demonstrated. PP has very poor miscibility with UHMWPE with tremendous UHMWPE particles and exhibits poor interfacial interdiffusion without effective entanglement network. From the perspective of the macromolecular chain segments probed by rheological measurement, the interfacial interdiffusion

force of UHMWPE is more significant regarding the two polyolefins containing polyethylene segments, leading to enhanced mechanical properties especially EPDM. EPDM possesses a higher maximum addition threshold concerning rheological and mechanical behaviors. UHMWPE cocrystallizes with EPDM with promoted aggregate structure, and the blend shows superior comprehensive mechanical properties especially Young's modulus. Therefore, low-entanglement UHMWPE particles can be regarded as an ideal reinforcing filler for metallocene polyolefins containing polyethylene segments to broaden their application fields. The key to enhancement is forming entanglements through efficient interfacial interdiffusion of polyethylene segments. This research provides a reference for designing the UHMWPE-reinforcing polymer. For example, polyethylene segments are expected to be introduced into the matrix by copolymerization or blending, helping UHMWPE perform a better enhancement effect.

Data Availability

The data that support the findings of this study are available on request from the corresponding authors. The data are not publicly available due to privacy or ethical restrictions.

Conflicts of Interest

The authors declared that they have no conflicts of interest to this work.

Authors' Contributions

Xin Tang and Jinheng Xing contributed equally to this work.

Acknowledgments

References

[1] C. T. Lue, "Easy processing metallocene polyethylene," *Journal of Plastic Film & Sheeting*, vol. 15, no. 2, pp. 131–139, 1999.

[2] W. Kaminsky and A. Laba, "Metallocene catalysis," *Applied Catalysis A: General*, vol. 222, no. 1-2, pp. 47–61, 2001.

[3] N. S. Allen, M. Edge, C. M. Liauw, and E. Hoang, "Role of phenol and phosphite antioxidant combinations in the thermal stabilisation of metallocene LLDPE (mLLDPE): optimisation and performance and influence of metal stearates on multiple extrusions," *Polymer Degradation and Stability*, vol. 152, pp. 208–217, 2018.

[4] M. Stürzel, S. Mihan, and R. Mülhaupt, "From multisite polymerization catalysis to sustainable materials and all-polyolefin

composites," *Chemical Reviews*, vol. 116, no. 3, pp. 1398–1433, 2016.

[5] C. H. Stephens, A. Hiltner, and E. Baer, "Phase behavior of partially miscible blends of linear and branched polyethylenes," *Macromolecules*, vol. 36, no. 8, pp. 2733–2741, 2003.

[6] M. Kontopoulou, W. T. Wang, C. Gopakumar, and C. Cheung, "Effect of composition and comonomer type on the rheology, morphology and properties of ethylene-α-olefin copolymer/polypropylene blends," *Polymer*, vol. 44, no. 24, pp. 7495–7504, 2003.

[7] S. Ratner, A. Pegoretti, A. Migliaresi, and G. Weinberg, "Relaxation processes and fatigue behavior of crosslinked UHMWPE fiber compacts," *Composites Science and Technology*, vol. 65, no. 1, pp. 87–94, 2005.

[8] Z. Li, W. Zhang, X. Wang, Y. Mai, and Y. Zhang, "Surface modification of ultra high molecular weight polyethylene fibers via the sequential photoinduced graft polymerization," *Applied Surface Science*, vol. 257, no. 17, pp. 7600–7608, 2011.

[9] S. Rastogi, D. R. Lippits, G. W. Peters, R. Graf, Y. Yao, and H. W. Spiess, "Heterogeneity in polymer melts from melting of polymer crystals," *Nature Materials*, vol. 4, no. 8, pp. 635–641, 2005.

[10] G. B. Shah and M. Fuzail, "Modification of polyethylene and incorporation of fillers for effective reinforcement of mechanical and better flame retardant properties," *Journal of Applied Polymer Science*, vol. 99, no. 4, pp. 1928–1933, 2006.

[11] A. Pandey, Y. Champouret, and S. Rastogi, "Heterogeneity in the distribution of entanglement density during polymerization in disentangled ultra-high-molecular-weight polyethylene," *Macromolecules*, vol. 44, no. 12, pp. 4952–4960, 2011.

[12] H. Shen, L. He, C. Fan, B. Xie, W. Yang, and M. Yang, "Effective dissolution of UHMWPE in HDPE improved by high temperature melting and subsequent shear," *Polymer Engineering & Science*, vol. 55, no. 2, pp. 270–276, 2015.

[13] T. Deplancke, O. Lame, F. Rousset, I. Aguili, R. Séguéla, and G. Vigier, "Diffusion versus cocrystallization of very long polymer chains at interfaces: experimental study of sintering of UHMWPE nascent powder," *Macromolecules*, vol. 47, no. 1, pp. 197–207, 2014.

[14] Y. Q. Xue, T. Tervoort, and P. Lemstra, "Welding behavior of semicrystalline polymers. 1. The effect of nonequilibrium chain conformations on autoadhesion of UHMWPE," *Macromolecules*, vol. 31, no. 9, pp. 3075–3080, 1998.

[15] H. Q. Yang, L. Hui, J. J. Zhang, P. Chen, and W. Li, "Effect of entangled state of nascent UHMWPE on structural and mechanical properties of HDPE/UHMWPE blends," *Journal of Applied Polymer Science*, vol. 134, no. 16, p. 44728, 2017.

[16] Y. M. Chen, P. Liang, Z. Yue et al., "Entanglement formation mechanism in the POSS modified heterogeneous Ziegler-Natta catalysts," *Macromolecules*, vol. 52, no. 20, pp. 7593–7602, 2019.

[17] P. Chen, H. Yang, T. Chen, and W. Li, "Weakly entangled ultra-high-molecular-weight-polyethylene prepared via ethylene extrusion polymerization," *Industrial & Engineering Chemistry Research*, vol. 54, no. 44, pp. 11024–11032, 2015.

[18] V. Divya, V. Pattanshetti, R. Suresh, and R. Sailaja, "Development and characterisation of HDPE/EPDM-g-TMEVS blends for mechanical and morphological properties for engineering applications," *Journal of Polymer Research*, vol. 20, no. 2, pp. 1–11, 2013.

[19] M. Ono, J. Washiyama, K. Nakajima, and T. Nishi, "Anisotropic thermal expansion in polypropylene/poly(ethylene-co-octene) binary blends: influence of arrays of elastomer domains," *Polymer*, vol. 46, no. 13, pp. 4899–4908, 2005.

[20] V. M. Egorov, E. M. Ivan'kova, V. A. Marikhin, L. P. Myasnikova, and A. Drews, "On fine structure of nascent UHMWPE reactor powders," *Journal of Macromolecular Science, Part B*, vol. 41, no. 4-6, pp. 939–956, 2002.

[21] E. C. L. Pereira, B. G. Soares, A. A. Silva, J. M. F. da Silva, G. M. Barra, and S. Livi, "Conductive heterogeneous blend composites of PP/PA12 filled with ionic liquids treated-CNT," *Polymer Testing*, vol. 74, no. 74, pp. 187–195, 2019.

[22] N. S. S. Kashani, F. Gharavani, N. Jaberi et al., "Influence of organoclay and nitroxylether on the rheological, thermal and flame-retardant properties of co-continuous PP/EVA blends," *Plastics, Rubber and Composites*, vol. 51, no. 6, pp. 306–315, 2022.

[23] H. Liu, X. Zhang, H. Suwardie, P. Wang, and C. G. Gogos, "Miscibility studies of indomethacin and Eudragit® E PO by thermal, rheological, and spectroscopic analysis," *Journal of Pharmaceutical Sciences*, vol. 101, no. 6, pp. 2204–2212, 2012.

[24] B. Wu, Y. Cai, X. Zhao, and L. Ye, "Fabrication of well-miscible and highly enhanced polyethylene/ultrahigh molecular weight polyethylene blends by facile construction of interfacial intermolecular entanglement," *Polymer Testing*, vol. 93, p. 106973, 2021.

[25] Y. M. Li, Y. Wang, L. Bai, H. L. Z. Zhou, W. Yang, and M. B. Yang, "Dynamic rheological behavior of HDPE/UHMWPE blends," *Journal of Macromolecular Science, Part B*, vol. 50, no. 7, pp. 1249–1259, 2011.

[26] C. L. P. Shan, J. B. Soares, and A. Penlidis, "HDPE/LLDPE reactor blends with bimodal microstructures–part II: rheological properties," *Polymer*, vol. 44, no. 1, pp. 177–185, 2003.

[27] Y. Li, H. He, Y. Ma, Y. Geng, and J. Tan, "Rheological and mechanical properties of ultrahigh molecular weight polyethylene/high density polyethylene/polyethylene glycol blends," *Advanced Industrial and Engineering Polymer Research*, vol. 2, no. 1, pp. 51–60, 2019.

[28] C. Liu, J. Wang, and J. He, "Rheological and thermal properties of m-LLDPE blends with m-HDPE and LDPE," *Polymer*, vol. 43, no. 13, pp. 3811–3818, 2002.

[29] L. P. Li, B. Yin, Y. Zhou et al., "Characterization of PA6/EPDM-g-MA/HDPE ternary blends: the role of core-shell structure," *Polymer*, vol. 53, no. 14, pp. 3043–3051, 2012.

[30] K. Chaudhuri and A. K. Lele, "Rheological quantification of the extent of dissolution of ultra-high-molecular-weight-polyethylene in melt-compounded blends with high density polyethylene," *Journal of Rheology*, vol. 64, no. 1, pp. 1–12, 2020.

[31] G. Tao, Y. M. Chen, J. S. Mu, L. T. Zhang, C. L. Ye, and W. Li, "Exploring the entangled state and molecular weight of UHMWPE on the microstructure and mechanical properties of HDPE/UHMWPE blends," *Journal of Applied Polymer Science*, vol. 138, no. 30, p. 50741, 2021.

[32] C. D. Han and J. K. Kim, "On the use of time-temperature superposition in multicomponent/multiphase polymer systems," *Polymer*, vol. 34, no. 12, pp. 2533–2539, 1993.

[33] M. Liu, Y. Wang, J. Chen, J. Luo, Q. Fu, and J. Zhang, "The retarded recovery of disentangled state by blending HDPE with ultra-high molecular weight polyethylene," *Polymer*, vol. 192, p. 122329, 2020.

[34] J. Chuang, A. Y. Grosberg, and T. Tanaka, "Topological repulsion between polymer globules," *The Journal of Chemical Physics*, vol. 112, no. 14, pp. 6434–6442, 2000.

[35] X. Zhang, S. Zhao, and Z. Xin, "The chain dis-entanglement effect of polyhedral oligomeric silsesquioxanes (POSS) on ultra-high molecular weight polyethylene (UHMWPE)," *Polymer*, vol. 202, p. 122631, 2020.

[36] L. Han, H. Xu, B. Wang et al., "Preparation and characterization of biodegradable poly(ϵ-caprolactone) self-reinforced composites and their crystallization behavior," *Polymer International*, vol. 66, no. 11, pp. 1555–1563, 2017.

[37] S. K. Pillai, V. Ojijo, and S. S. Ray, "Crystallization and thermal properties of polylactide/palygorskite composites," *Journal of Applied Polymer Science*, vol. 131, no. 12, 2014.